Delft University of Technology

A control-oriented wind turbine dynamic simulation framework which resolves local atmospheric conditions

Feng, Z.; Ferrari, R.; van Wingerden, J. W.; Liu, Y.

Important note
To cite this publication, please use the final published version (if applicable).
Please check the document version above.

A control-oriented wind turbine dynamic simulation framework which resolves local atmospheric conditions

Z. Feng & R. Ferrari & J.W. van.Wingerden
Delft Center of System and Control,Delft University of Technology, Delft, Netherlands

Y. Liu
Electric Power Research Institute (Europe), Dublin, Ireland

ABSTRACT: Wind turbines may experience local weather perturbation, which is not taken into account by the commonly-used wind turbine simulation packages. Without this information, it is extremely challenging to evaluate the controller performance with regard to the effect of the variation of local atmospheric conditions. On the other side, it is too late and costly to wait until field test time. To fill this gap, in this paper, we develop a control-oriented turbine dynamic simulation framework to evaluate the controller performance considering the perturbation of local atmospheric conditions. This goal is achieved by integrating an internal wind turbine (IWT) model in the Weather Research and Forecasting (WRF) simulation tool. The proposed framework is implemented on a 5MW reference wind turbine, where the effects of the local atmospheric conditions are illustrated. The proposed WRF-IWT model are validated by comparing the results with those derived from the Fatigue, Aerodynamics, Structures, and Turbulence (FAST).

1 INTRODUCTION

In past decades, wind energy has received an increasing attention in the international energy market. This motivates more research on developing efficient wind turbine controller to optimize power generation and alleviate structural loads. However, it remains a challenge to simulate the generated power and the structural loads in real-world conditions, due to the complex time-varying meteorological phenomena that are involved. In addition, there is a lack of simulation tools oriented to wind turbine control that can account for the local atmospheric conditions during the controller design process. Finally, waiting for field tests to evaluate the influence of such local conditions on controller performance is neither timely, nor economically convenient. Therefore, there is an urgent need to develop a control-oriented numerical approach to simulate the interaction of a wind turbine with local atmospheric effects.

The generalized actuator disk (GAD) and the generalized actuator line (GAL) are two widely used turbine models to compute the aerodynamic loads under a given incoming flow field (Boersma et al. 2017). To capture the aerodynamic performance, they are integrated with the flow model in control-oriented numerical simulation tools, such as the Simulator for Wind Farm Applications (SOWFA) (Churchfield et al. 2012) and the Flow Redirection and Induction in Steady-state (FLORIS) (Gebraad et al. 2016) numerical model. Although very effective, these models usually assume that the vertical shape of the wind flow can be ideally approximated by the uniform, power law, logarithmic wind profile models or a given boundary condition (Sharma et al. 2018). However, such an assumption is not always valid when a wind farm experiences short-term local weather perturbation (Liu et al. 2017). This, due to the lack of the atmospheric information, will lead to the sub-optimal design of the control system of the wind turbine. Thus, the designed controller based on these simulation tools might be less applicable for the wind turbine operating in the real world (Rai et al. 2017).

To consider a condition which is more representative of actual ones, the wind field can be derived by a physics-based model. Weather Research and Forecasting (WRF) is an advanced atmospheric prediction system that integrates fully compressible, non-hydrostatic Euler equations (Skamarock et al. 2021). The solver of WRF has the ability to resolve the flow around the wind turbine in a realistic, time-varying atmospheric environment. For this reason the wind field solution produced by WRF is widely used in SOWFA as an initial condition (Churchfield et al. 2013, Maché, M. et al. 2014). A WRF based large eddy simulation (LES) model with control strategies

was developed to consider the local atmospheric condition above complex terrains in (Wang et al. 2020). A control-oriented LES model was designed to simulate the wind turbine wake, considering the Coriolis force, in (Qian et al. 2022). Nevertheless, these numerical simulation methods use a one-directional coupling from the flow to the turbine, where the effects that turbines have on the surrounding wind field are not be considered. Thus, the finer details of the actual atmospheric conditions around turbines cannot be resolved.

To derive a more accurate atmospheric conditions, in previous literature a turbine simulator is developed by two-way coupling between a turbine model and WRF-GAD model is integrated in the WRF code (Mirocha et al. 2014). The proposed model is able to simulate the turbine aerodynamic performance in realistic atmospheric condition. Nevertheless, it simplifies the model of rotation speed of the turbine by a piece-wise linear function versus wind speed, where the generator dynamics and control law are not captured. Thus, it leads to a limited capability of serving for control-oriented simulation in realistic atmospheric conditions. In addition, both the WRF-GAD model and the WRF-LES models mentioned above are not able to consider the turbine structural dynamics model. Thus, they are not able to simulate the turbine structural vibration and capture its effects, such as the influence of the relative wind speed at the rotor due to the tower movement.

To fill this gap, in this paper we develop a control-oriented wind turbine dynamic simulation framework which can be used to validate a given control design under local atmospheric conditions. This goal is achieved by integrating an internal wind turbine (IWT) model in the Weather Research and Forecasting (WRF) simulation tool. WRF is a physics-based meteorological simulation tool, which is capable of generating a variety of local atmospheric characteristics by a series of parameterized physical schemes. Thus, it is able to simulate the perturbation of local atmospheric conditions. In addition, the IWT model includes a generalized actuator disk (GAD) model, drive-train dynamics and a tower top vibration model. It is then integrated in WRF such that the turbine and control dynamics under the time-varying local atmospheric conditions can be taken into account. We employ the proposed model to numerically simulate a 5MW wind turbine developed by the US National Renewable Energy Laboratory (NREL) (Jonkman et al. 2009). The turbine is situated in the sea, near the Oceanic Platform of the Canary Islands (PLOCAN) site. The effects of the local atmospheric conditions are illustrated on the 5MW turbine with a BTC. Simulation results show that the proposed WRF-IWT model is able to capture the turbine dynamics and controller performance regarding the perturbation of the complex local atmospheric conditions. The results of controller performance are compared to those

derived from the Fatigue, Aerodynamics, Structures, and Turbulence (FAST) simulator. The comparison validates that the drive-drain dynamics and controller work properly in the proposed WRF-IWT model. The results show significant potential for using the proposed framework to develop and validate wind turbine control law under time-varying realistic atmospheric conditions.

The remainder of this paper is organized as follows: Section 2 outlines the theoretical framework of WRF and GAD models. Section 3 introduces the tower top vibration model, where its effects on the relative wind speed is elaborated. In Section 4, a case study is carried out to exhibit its potential for controller design and to verify the results. Finally, conclusions are drawn in Section 5.

2 NUMERICAL MODEL

This section introduces the theoretical framework of the GAD model developed in WRF, the drive-train dynamics and the BTC algorithms.

2.1 *WRF-GAD Model*

The schematic of GAD model in presented in Fig.1, where x is the stream-wise direction aligned with the incoming wind speed V_0. V_1 is the velocity normal to the disk, which is reduced from its upstream value as a result of the widening of the stream tube. The induction factor a_{n} is introduced to account for this effect, then we have:

$$V_1 = V_0(1 - a_{\mathrm{n}}).$$

A similar expression can be derived for the downstream velocity V_2 based on Bernoulli's equation (Burton et al. 2011) as:
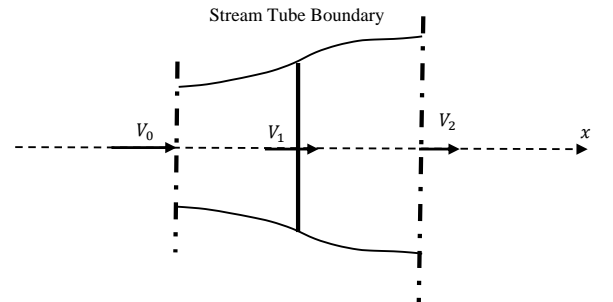
$$V_2 = V_0(1 - 2a_{\mathrm{n}}).$$

Figure 1: GAD model schematic.

In GAD model, the turbine blades are represented by a rotating disk model, where the lift and drag forces are calculated based on the blade element theory (Burton et al. 2011). The forces and angles on an

airfoil section are presented in Fig.2. The relation of the angles then is derived by:

$$\beta = \psi - \alpha - \xi,$$

where β is the pitch angle, α is the angle of attack, ψ is the advance angle, ξ is the twist angle. The lift F_L and drag F_D produced by the wind can be derived (Manwell et al. 2002) as:

$$F_L = \frac{1}{2}\rho V_r^2 c C_l$$
$$F_D = \frac{1}{2}\rho V_r^2 c C_d \tag{1}$$

where ρ is the air density, V_r is the relative wind speed over the airfoil, c is the the chord length of the blade, and C_l and C_d are the coefficients of lift and drag, respectively.
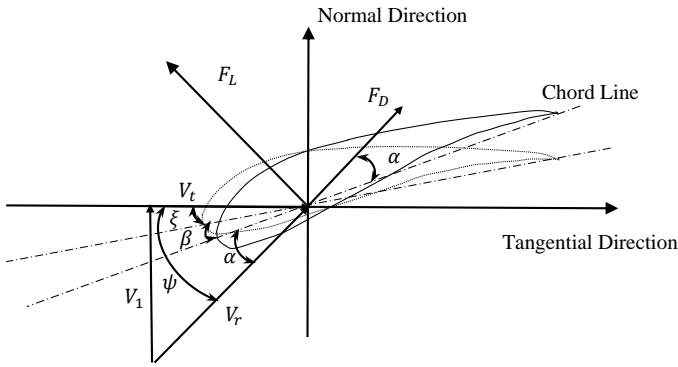

Figure 2: Forces and angles on an airfoil section, where α is the advance angle, V_r is the relative wind speed.

Then the axial force F_n and the tangential force F_t of each unit length can be derived by:

$$F_n = F_L \cos\psi + F_D \sin\psi$$
$$F_t = F_L \sin\psi - F_D \cos\psi \tag{2}$$

The projection of $\mathrm{d}F_n$ and $\mathrm{d}F_t$ onto the $[x,y,z]$ coordinate system in presented in Fig.3. The relations can be derived (Mirocha et al. 2014) as:

$$F_x = F_n \cos\Phi + F_t \sin\zeta \sin\Phi$$
$$F_y = F_n \sin\Phi - F_t \sin\zeta \cos\Phi, \tag{3}$$
$$F_z = -F_t \cos\zeta$$

where Φ and ζ describe the orientation of P on the actuator disk with respect to $[x,y,z]$ coordinate system in WRF. Then F_x, F_y and F_z are added to the momen-
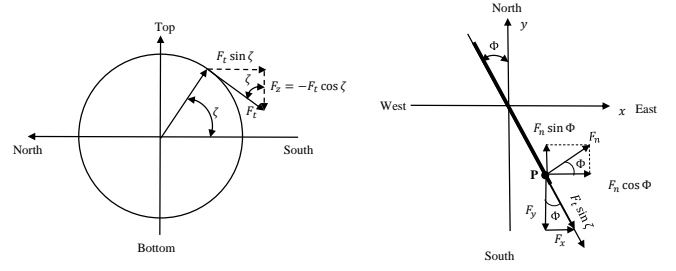

Figure 3: The projection of $\mathrm{d}F_n$ and $\mathrm{d}F_t$ onto the $[x,y,z]$ coordinate system in WRF

tum equation in WRF (Mirocha et al. 2014) as:

$$\frac{\partial u}{\partial t} = -\frac{1}{2\pi r\rho}G\left(d_n\right)F_x$$
$$\frac{\partial v}{\partial t} = -\frac{1}{2\pi r\rho}G\left(d_n\right)F_y \tag{4}$$
$$\frac{\partial w}{\partial t} = -\frac{1}{2\pi r\rho}G\left(d_n\right)F_z,$$

where u, v, and w are the the three components of velocities. And $G\left(d_n\right)$ is a normal distribution, which is used to avoid numerical instabilities due to the strong forces applied at isolated grid points. $G\left(d_n\right)$ is with 0 mean and a standard standard deviation that is set to be the grid size.

Based on the above momentum analysis, F_t is derived by Eq.(2). Then the aerodynamic power P_r is defined as:

$$P_r = \sum F_t r\, dr. \tag{5}$$

Then we can derived T_r by:

$$T_r = P_r/\omega_r.$$

2.2 Drive Train Dynamics

For the WT dynamics, we model the turbine, drive-train and generator as a single rotational system, with generator speed ω_g in rad/s, and rotor speed $\omega_r(t) = \omega_g/N$ in rad/s, where N is the gear ratio of the drive-train. We let J_g and J_r denote the inertia of the generator and rotor, respectively, and we let $J = J_g + J_r/N^2$ denote the equivalent inertia at the generator shaft. Neglecting losses, the dynamics is given by (Hovgaard et al. 2015) as:

$$J\dot\omega_g(t) = T_r(t)/N - T_g(t),$$

where $T_r(t)$ and $T_g(t)$ are the rotor and generator torque, respectively.

2.3 Baseline Torque Control Algorithms

Then we develop the BTC based on the $K\omega^2$ torque control law (Jonkman et al. 2009) as:

$$\tau_g = K\omega_r^2/N, \tag{6}$$

where τ_{g} is the generator torque. $K \in \mathbb{R}^+$ is the optimal mode gain derived by.

$$K = \frac{\pi \rho R^5 C_{\mathrm{p}}(\lambda, \beta)}{2\lambda^3},$$

where R is the rotor radius, β is the blade pitch angle, v_w is the wind speed, λ is the tip-speed ratio. C_p is the power coefficient, which can be derived from a lookup table.

3 WRF-IWT MODEL

In this section, the tower vibration model in WRF-IWT framework is introduced, as well as its influence on the relative wind speed between the rotor and the inflow wind.

3.1 *Tower Top Vibration Model in WRF*

The thrust on an annular cross-section $\mathrm{d}T$ can be determined by the following expression that uses a_{n} (Mirocha et al. 2014, Manwell et al. 2002) as:

$$\mathrm{d}T = BF_{\mathrm{n}}\mathrm{d}r, \tag{7}$$

where F_{n} is derived by Eq. (2), B is the number of blades, which equals to 3. Then the total thrust force T is calculated as:

$$T = \sum \mathrm{d}T. \tag{8}$$

The dynamics of the fore-aft bending mode of the tower is modeled as a second-order system as Eq.(9) (Shaltout et al. 2017):

$$M_{\mathrm{T}}\ddot{x}_{\mathrm{T}} + B_{\mathrm{T}}\dot{x}_{\mathrm{T}} + K_{\mathrm{T}}x_{\mathrm{T}} = T, \tag{9}$$

where x_{T} is the fore-aft displacement of the tower top, and M_{T}, B_{T} and K_{T} are the tower equivalent mass, structural damping, and bending stiffness, respectively.

3.2 *Interaction between Tower Vibration and Inflow Wind*

To construct an accurate turbine simulation approach, it is important to consider the effects on relative wind speed due to the turbine vibration. As shown in Fig. 4, the tower fore-after vibration $\vec{V}_{\mathrm{fa}}$ is along the axial of the turbine, the same direction as $\vec{V}_{\mathrm{r}}$. Then we can derive the actual relative wind speed $\vec{V}_{\mathrm{ac}}$ as:

$$\vec{V}_{\mathrm{ac}} = \vec{V}_{\mathrm{r}} + \vec{V}_{\mathrm{fa}}. \tag{10}$$

Then the $\vec{V}_{\mathrm{ac}}$ is used in Eq.(2) to derive more accurate nominal and tangential forces. Then based on Eq.(5) and Eq.(7), power and thrust force are derived.

Based on this WRF-IWT model, the proposed framework is able to take into consideration of the effect of the tower vibration on the aerodynamics loads and power production.
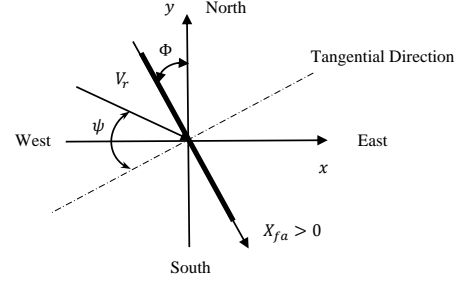

Figure 4: The relation between WRF and tower vibration coordination

4 SIMULATION

In this section, the performance of the proposed numerical simulation framework is exhibited on the NREL 5MW reference wind turbine with BTC. In section A and B, the turbine parameters and WRF configuration are introduced, respectively. In section C, the results derived by the WRF-IWT framework are presented, which are used to verify the BTC performance under local atmospheric conditions near PLOCAN site. The results are also analyzed by being compared with those derived from FAST.

4.1 *Wind Turbine Configuration*

The wind turbine is situated in the PLOCAN site. The parameters of NREL-5MW wind turbine model are listed in Table 1. The tower top vibration model is constructed based on the natural frequency f_1 and the damping ratio d_1 of the first fore-aft vibration mode, based on Eq.(9).

4.2 *WRF Configuration*

The wind turbine is situated in the PLOCAN site. The reanalysis data from the Global Forecast System (GFS) (National Centers for Environmental Prediction, National Weather Service, NOAA, U.S. Department of Commerce 2015) are used as initial/boundary conditions. They are derived from high-resolution forecasts in both spatial and temporal spaces.

The resolution of the GFS data set is on a 0.25 by 0.25 degree global latitude longitude grid, which is around 30×30 km. With the WRF Preprocessing System (WPS), the GFS input data can be interpolated to the horizontal grid spacing of 2250×2250 km. Then it is designed to be the first domain. A 5-domain nesting method is implemented to provide the grid scale fit for the individual turbine simulation. The details of the nesting method are presented in Table 3. This nesting method is designed according to the nesting strategy and analysis in Talbot et al. (2012). The The wind turbine locates in the 5th domain, where the horizontal grid size is set to be 10 meters. The first two domains are used for mesoscale simulations, while the finest three are used for the large-eddy simulation (LES) technique to simulate the turbine aerody-

Table 1: The parameters of NREL 5 MW wind turbine model (Jonkman et al. 2009).

Parameter	Magnitude
Rated power, $P_{g,rated}$	5 MW
Rotor diameter, D_r	126 m
Tower height, H_t	87.5 m
Cut-in wind speed	3 m/s
Cut-out wind speed	25 m/s
Rated wind speed	11.4 m/s
Rated generator speed, $\omega_{g,rated}$	122.9096 rad/s
Minimum generator speed, $\omega_{g,\,min}$	41.6470 rad/s
Maximum generator speed, $\omega_{g,\,max}$	159.7824 rad/s
Maximum generator torque, T_g	4.3094×10^4 N·m
Generator efficiency, η	0.9440
Gear ratio, G	97
Rotor Inertia, J_r	35,444,067 kg/m^2
Generator inertia, J_g	534.116 kg/m^2
Optimal tip-speed ratio, λ^0	7.6
Optimal blade pitch angle, β^0	0 deg
Maximum power coefficient, $C_{p,\,max}$	0.4868
Mass nacelle, M_N	240000 kg
Mass hub, M_H	56780 kg
Mass blade, M_B	17848.770 kg
1st tower fore-Aft natural frequency, f_1	0.3240 Hz
1st mode damping ratio, d_1	1%

namics performance. Therefore, the Mellor-Yamada-Janjic (MYJ) scheme is selected as planetary Boundary layer (PBL) of the first 2 domains, while the LES is selected for the finer 3 domains. Here, MYJ scheme is an Eta operational scheme, which is a one-dimensional prognostic turbulent kinetic energy scheme with local vertical mixing (Peckham et al. 2017). The Grell scheme is only used in the coarsest domain because in a clear day the scheme is not relevant (Talbot et al. 2012). The Smagorinsky closure is chosen as it is recommended for real-data case (Peckham et al. 2017). More details of physics options used for the five domains are presented in Table 2.

The simulations last for 180 seconds. The first 60s are truncated to avoid the instability at the beginning periods. The output data from WRF is derived every second.
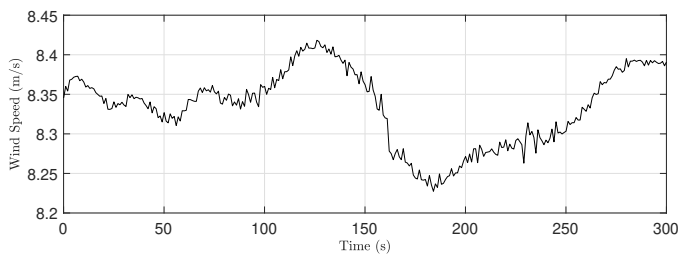
4.3 *Results and Discussion*

Figure 5: Wind speed at the hub height.

The wind speed at the hub height is presented in Fig. 5. To get a knowledge of the wind profile around the disc area, the wind field in the vertical plane around the turbine at $t = 90$ is presented in Fig. 6. In Fig. 6(a), the positive value refers to the north direction; In Fig. 6(b), the positive value refers to the east direction;In Fig. 6(c), the positive value refers to the upper direction. As shown in Fig. 6, the wind speed varies in the overall disk district. Besides, the proposed WRF-IWT model is able to capture the wakes dynamics. In Fig. 7, the horizontal view of wakes at hub height is presented. As shown in Fig. 6-Fig. 7, the proposed WRF-IWT model is able to capture the turbine's influence on the surrounding wind field, as well as the wake influence.

In addition, the proposed WRF-IWT model has the capability to simulate the turbine dynamics and controller performance. Under the wind condition presented in Fig. 5, the wind speed is below the rated wind speed 11.4 m/s. Thus, the BTC is activated (Jonkman et al. 2009). In Fig. 8, the controller performance is presented and compared with results derived from FAST. In Fig. 8(a), the comparison of the captured rotor power P_r is presented. As shown in the plot, it matches quite well with the results derived by FAST. Besides, it is able to capture the time-varying variation of P_r caused by the local atmospheric perturbation and the tower vibration. Nevertheless, with the BTC this variation does not affect the smooth of generator power production P_g, ω_g and T_g, as shown in Fig. 8(b)-Fig. 8(d). Thus, the proposed WRF-IWT model is able to simulate the two-way coupling between the local atmospheric and the turbine with BTC locating inside that area. Besides, it

Table 2: Physics setting of each domain in WRF.

Domain	PBL scheme	Land surface model	Closure	Cumulus Parameterization	Radiation
1	MYJ	NJSM	Smagorinsky	Grell scheme	RRTM
2	MYJ	NJSM	Smagorinsky	-	RRTM
3	LES	NJSM	Smagorinsky	-	RRTM
4	LES	NJSM	Smagorinsky	-	RRTM
5	LES	NJSM	Smagorinsky	-	RRTM

*NJSM: Noah Land Surface Model; RRTM: Rapid Radiative Transfer Model.

*The Radiation includes both longwave and shortwave radiation.

Table 3: Grids nesting design in WRF.

	nx	ny	dx/m	dy/m	Lx/km	Ly/km
1	105	105	2250	2250	236.25	236.25
2	103	103	750	750	7725	77.25
3	101	101	150	150	15.15	15.15
4	201	201	30	30	6.03	6.03
5	301	301	10	10	3.01	3.01

(a) U component (b) V component

(c) W component (d) Total wind speed
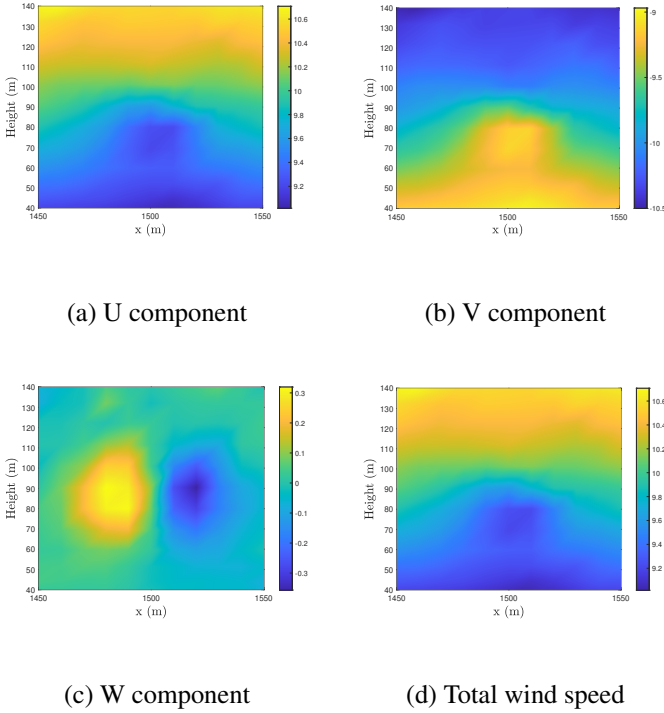
Figure 6: Wind field around the GAD region, at $t = 90$ s.
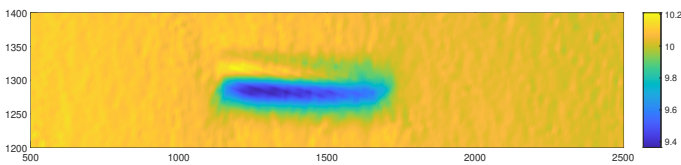
Figure 7: Wind turbine wake at the hub height, in the horizontal plane, at $t = 90$ s.

also provide an insight of the BTC performance under the local atmospheric conditions with time-varying perturbation. At the same time, in general they also match the results derived by FAST. Because the proposed WRF-IWT model uses a simplified drive-train model. It is reasonable that the results do not match perfectly but have some minor differences. Therefore, the dynamics and controller in the proposed WRF-IWT model is validated to work properly.

Furthermore, based on the model in Section III.B, the proposed framework is able to simulate the tower vibration under short-term realistic local atmospheric conditions. The results are presented in Fig.9, where V_{fa} and A_{fa} are the tower top vibration velocity and acceleration, respectively. As shown in Fig.9(a), the thrust force is influenced by the perturbation of local atmosphere and tower vibration, which shows a similar tendency as the P_{r}. Besides, as shown in Fig. 9(b)-Fig. 9(c), the tower vibration dynamics is also captured, which indicates that it is also influenced by the local wind perturbation. Thus, it is able to capture the tower vibration dynamics affected by the local atmospheric perturbation. This provides important information for further controller development with tower fatigue load mitigation.

In summary, the proposed WRF-IWT model is capable to capture the influence of a turbine with BTC on the local wind conditions, as well as the turbine dynamics influenced by the local atmospheric perturbation. Thus, it achieves to simulate the two-way coupling interaction between the local atmospheric conditions and a turbine with BTC. The simulation results not only provides an insight of the important information, but also show a potential of the proposed model to assist power optimization and tower fatigue load reduction controller development.
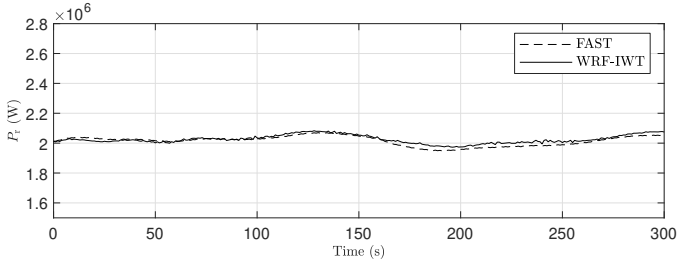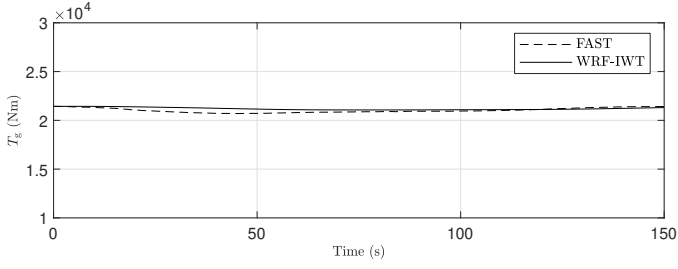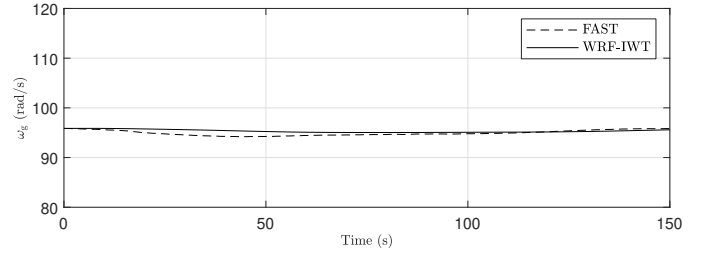
(a) Comparison of the rotor power P_r.
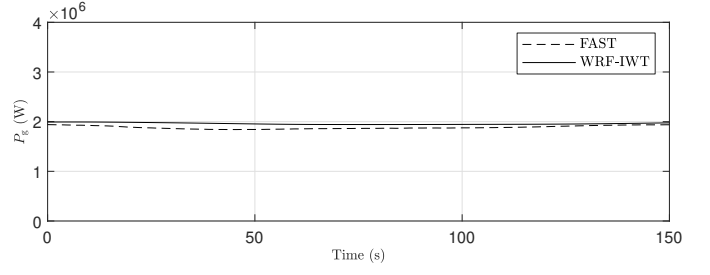
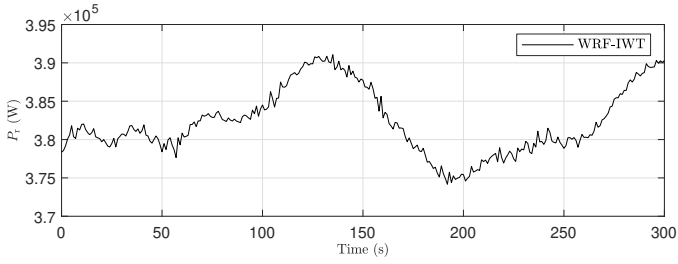

(b) Comparison of the generator power P_g.

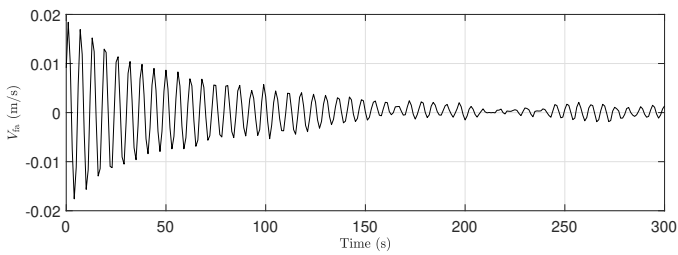(c) Comparison of the generator torque T_g.

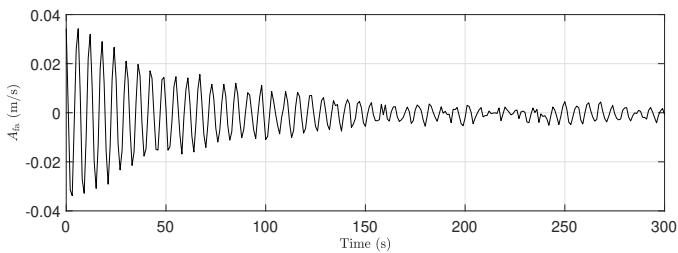(d) Comparison of the generator rotation speed ω_g.

Figure 8: Comparison of the control performance between the WRF-IWT framework and the FAST model.

(a) The thrust force T captured by the WRF-IWT model.

(b) WRF-IWT: tower top velocity V_fa.

(c) WRF-IWT: tower top acceleration A_fa.

Figure 9: Tower top vibration simulated via the WRF-IWT framework.

5 CONCLUSIONS

In this paper, we develop a control-oriented wind turbine dynamic simulation framework considering time-varying local atmospheric conditions. This is achieved by integrating an internal wind turbine (IWT) model in the weather research and forecast (WRF) simulation tool. The IWT is composed of a generalized actuator disk (GAD) model, the drive-train dynamics and a tower top vibration model. The GAD model and drive-train dynamics developed in WRF enables it to simulate the turbine dynamics and controller performance under short-term local atmospheric condition. By introducing the tower top vibration model, the proposed framework is able to capture the tower top motion and its effect on the relative wind speed between the rotor and the inflow wind speed. The proposed WRF-IWT framework is employed to verify the performance of a baseline torque controller (BTC) on the National Renewable Energy Laboratory (NREL) 5MW reference wind turbine situated near PLOCAN site. Simulation results illustrate that the WRF-IWT model is able to simulate the wind turbine and control dynamics where the local atmospheric condition around the PLOCAN site is considered. The results derived from the WRF-IWT model matches well with those derived from the Fatigue, Aerodynamics, Structures, and Turbulence (FAST) simulator. Thus, the proposed framework shows high potential in assisting developing more applicable controllers for the wind turbine operating in the real world conditions, for both power optimization and tower fatigue load reduction objectives. Besides, in further research the current WRF-IWT framework has the potential to

be extended to consider sea wave effects for simulation of offshore wind turbines.

ACKNOWLEDGMENTS

REFERENCES

Boersma, S., B. Doekemeijer, P. Gebraad, P. Fleming, J. Annoni, A. Scholbrock, J. Frederik, & J.-W. van Wingerden (2017). A tutorial on control-oriented modeling and control of wind farms. In *2017 American Control Conference (ACC)*, pp. 1–18.

Burton, T., N. Jenkins, D. Sharpe, & E. Bossanyi (2011). *Wind energy handbook*. John Wiley & Sons.

Churchfield, M. J., S. Lee, J. Michalakes, & P. J. Moriarty (2012). A numerical study of the effects of atmospheric and wake turbulence on wind turbine dynamics. *Journal of Turbulence 13*, N14.

Churchfield, M. J., J. Michalakes, B. Vanderwende, S. Lee, M. A. Sprague, J. K. Lundquist, & P. J. Moriarty (2013). Using mesoscale weather model output as boundary conditions for atmospheric large-eddy simulations and wind-plant aerodynamic simulations (presentation). Technical Report PR-5000-61122, NREL.

Gebraad, P. M. O., F. W. Teeuwisse, J. W. van Wingerden, P. A. Fleming, S. D. Ruben, J. R. Marden, & L. Y. Pao (2016). Wind plant power optimization through yaw control using a parametric model for wake effects—a cfd simulation study. *Wind Energy 19*(1), 95–114.

Hovgaard, T. G., S. Boyd, & J. B. Jørgensen (2015). Model predictive control for wind power gradients. *Wind Energy 18*(6), 991–1006.

Jonkman, J., S. Butterfield, W. Musial, & G. Scott (2009, February). Definition of a 5-MW Reference Wind Turbine for Offshore System Development. Technical Report TP-500-38060, 947422, NREL.

Liu, Y., D. Chen, Q. Yi, & S. Li (2017). Wind profiles and wave spectra for potential wind farms in south china sea. part i: Wind speed profile model. *Energies 10*(1).

Maché, M., Mouslim, H., & Mervoyer, L. (2014). From meso-scale to micro scale les modelling: Application by a wake effect study for an offshore wind farm. *ITM Web of Conferences 2*, 01004.

Manwell, J., J. McGowan, & A. Rogers (2002, April). *Wind Energy Explained*. Chichester, UK: John Wiley & Sons, Ltd.

Mirocha, J. D., B. Kosovic, M. L. Aitken, & J. K. Lundquist (2014). Implementation of a generalized actuator disk wind turbine model into the weather research and forecasting model for large-eddy simulation applications. *Journal of Renewable and Sustainable Energy 6*(1), 013104.

National Centers for Environmental Prediction, National Weather Service, NOAA, U.S. Department of Commerce (2015). Ncep gdas/fnl 0.25 degree global tropospheric analyses and forecast grids.

Peckham, S., G. Grell, S. McKeen, R. Ahmadov, K. Wong, M. Barth, G. Pfister, C. Wiedinmyer, J. Fast, W. Gustafson, et al. (2017). Wrf-chem version 3.8.1 user's guide. Technical report.

Qian, G.-W., Y.-P. Song, & T. Ishihara (2022, January). A control-oriented large eddy simulation of wind turbine wake considering effects of Coriolis force and time-varying wind conditions. *Energy 239*, 121876.

Rai, R. K., H. Gopalan, J. Sitaraman, J. D. Mirocha, & W. O. Miller (2017, August). A code-independent generalized actuator line model for wind farm aerodynamics over simple and complex terrain. *Environmental Modelling & Software 94*, 172–185.

Shaltout, M. L., Z. Ma, & D. Chen (2017, 12). An Adaptive Economic Model Predictive Control Approach for Wind Turbines. *Journal of Dynamic Systems, Measurement, and Control 140*(5). 051007.

Sharma, V., G. Cortina, F. Margairaz, M. Parlange, & M. Calaf (2018, January). Evolution of flow characteristics through finite-sized wind farms and influence of turbine arrangement. *Renewable Energy 115*, 1196–1208.

Skamarock, W. C., J. B. Klemp, J. Dudhia, D. O. Gill, Z. Liu, J. Berner, W. Wang, J. G. Powers, M. G. Duda, D. M. Barker, & X.-Y. Huang (2021). A Description of the Advanced Research WRF Model Version 4. Technical Report TN-556+STR, NCAR.

Talbot, C., E. Bou-Zeid, & J. Smith (2012). Nested mesoscale large-eddy simulations with wrf: Performance in real test cases. *Journal of Hydrometeorology 13*(5), 1421 – 1441.

Wang, Q., K. Luo, R. Yuan, S. Wang, J. Fan, & K. Cen (2020, July). A multiscale numerical framework coupled with control strategies for simulating a wind farm in complex terrain. *Energy 203*, 117913.